

Mechanical behavior of δ -phase Pu–Ga alloys. Part II: Model verification and application

G.C. Kaschner *, M.G. Stout, S.S. Hecker

Materials Science and Technology Division, Los Alamos National Laboratory, MS G756, Los Alamos, NM 87545, USA

Received 5 July 2005; accepted 24 October 2005

Abstract

We validated the mechanical threshold strength (MTS) model, developed in Part I, with approximately 50 different experimental results from the literature for both yield strength and ultimate tensile strength on Pu–Ga alloys. One standard deviation of the differences between the model's yield-strength predictions and the experiments was 7.5% of the measured yield strength. The model also worked well predicting the ultimate tensile strength (UTS) of the alloys with gallium concentrations of 1 wt% or greater, although the accuracy of the UTS predictions was not as good as for yield strength. After validating the model, we studied the effects of gallium concentration, grain size, iron and nickel content, and carbon concentration on the yield strength of Pu–Ga alloys. The gallium concentration affected the yield strength more than any other microstructural variable. The yield strength increased 50% between 1 at.% Ga and 5.4 at.% Ga alloying addition. The grain size also produced a measurable strengthening effect, typical of other face-centered cubic metals. The yield strength increased 15% with a reduction in grain size from 50 μm to 10 μm . Finally, we found that there were no observable yield-strength effects resulting from different amounts of iron, nickel, or carbon impurities.

© 2005 Elsevier B.V. All rights reserved.

1. Introduction

In Part I, we evaluated the mechanical threshold strength (MTS) constitutive model of Follansbee and Kocks [1] for the δ -phase Pu–Ga alloy system. In Part II, we validate the model against 50 different experiments reported in the literature – mostly from

the 1960s and 1970s before the MTS model was developed – and use the model to predict the effects of gallium concentration, grain size, and various impurities on the yield and ultimate strengths of δ -phase Pu–Ga alloys.

These literature data represent alloys with a variety of microstructures – resulting from different alloy chemistries and thermomechanical processing methods – subjected to various test conditions – stress state, temperature, and strain rate – as summarized in Table 1 of Part I. Only a few of the references report uniaxial stress/strain curves. These data along with the torsion data of Wheeler

DOI of original article: [10.1016/j.jnucmat.2005.10.017](https://doi.org/10.1016/j.jnucmat.2005.10.017)

* Corresponding author. Tel.: +1 505 606 0107; fax: +1 505 667 8021.

E-mail address: kaschner@lanl.gov (G.C. Kaschner).

and Robbins [2] were used to determine the MTS-model parameters for Pu–Ga alloys. To validate the model, we compare predictions of the model to uniaxial yield and ultimate strengths as Hecker and Morgan [3], Miller and White [4], Beitscher [5], and Hecker [6] report.

However, first we comment on a few important microstructural considerations for Pu–Ga alloys. Gallium microsegregation resulting from coring during cooling through the $\delta + \epsilon$ two-phase field is common in Pu–Ga alloys [7]. The low-gallium areas are quite likely to transform to the hard, brittle α -phase during cooling or subsequent deformation. Robbins [8] points out that microsegregation likely contributed to much of the scatter in mechanical properties reported in the literature. An extended homogenization anneal at 450–470 °C can minimize gallium microsegregation. We selected those data from the literature that represented adequately homogenized δ -phase Pu–Ga alloys. However, it is important to stay within the limits of the temperature and pressure (or stress) stability of the alloys. For example, lean δ -phase plutonium alloys transform readily to the α -phase (with a corresponding 20% volume change) at subzero Celsius temperatures and pressures of a few tenths of a GPa [9]. Hence, it is important to check for temperature-induced transformations or stress-assisted and strain-induced transformations.

The results reported in the literature represent a range of grain sizes and sample purities – from high-purity electrorefined alloys, typically containing <200 ppm metallic impurities, to low-purity alloys, with as much as 2000 ppm total impurities. Impurities such as aluminum, silicon, and americium are present substitutionally in the lattice and, hence, have δ -phase stabilizing effects similar to gallium [7]. These impurity concentrations are simply added to the amount of gallium in the alloy on the basis of their atomic fraction present. Impurities such as carbon, oxygen, and nitrogen have no solubility and form hard, refractory inclusions, typically of micron size. We will focus on carbon in this study because it is one of the most common impurities in Pu–Ga alloys and it is widely reported in the literature. Iron and nickel are also common impurities in Pu–Ga alloys. At concentrations > 250 ppm, these elements form micron-size, low-melting intermetallic inclusions – either Pu₆Fe, Pu–Ni, or some combination – at grain boundaries or triple points [7,8].

2. Validation

As shown in Fig. 1, the yield strengths reported in the literature vary between 50 MPa and 130 MPa depending on the microstructure and testing conditions, a difference of 260%. Even for a single alloy of fixed composition and grain size – Beitscher’s data, for example – the yield strength is found to vary by 50% depending on strain rate and test temperature. Fig. 2 illustrates that we were able to reduce the experimental variation in yield strength in the literature data by applying the MTS model, which accounts for different test conditions and microstructural variables. We normalized the experimental yield-strength data by the MTS model’s prediction for temperature, strain rate, alloy composition, and grain size. In Fig. 2, the normalized yield strength is plotted versus the sum of gallium plus substitutional impurity content. The experimental data scatter about a horizontal line of value one. As shown in Fig. 2, ± 1 standard deviation of these data is only $\pm 7.5\%$; that is, 67% of the model’s predictions lie within 7.5% of the corresponding yield strength. The reader should note that the vertical scale of Fig. 2, although normalized, is equivalent to Fig. 1, giving a true sense of the degree to which the model collapses the data.

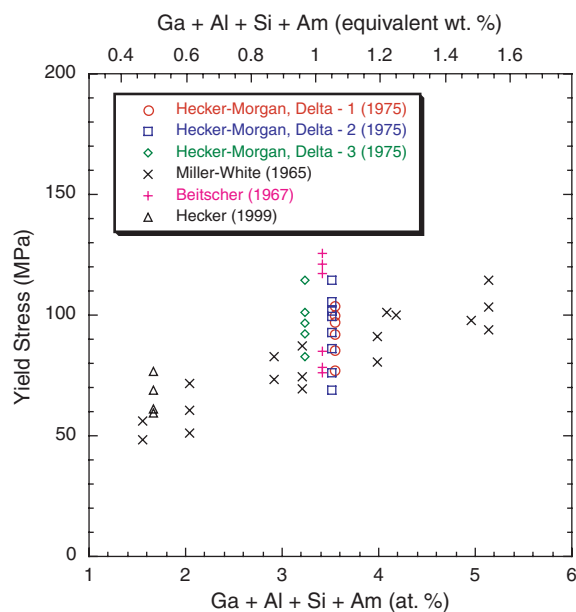


Fig. 1. Collection of uniaxial yield-stress data for δ -phase Pu–Ga alloys from the published literature. The scatter in these data reflects variations in test conditions and microstructures.

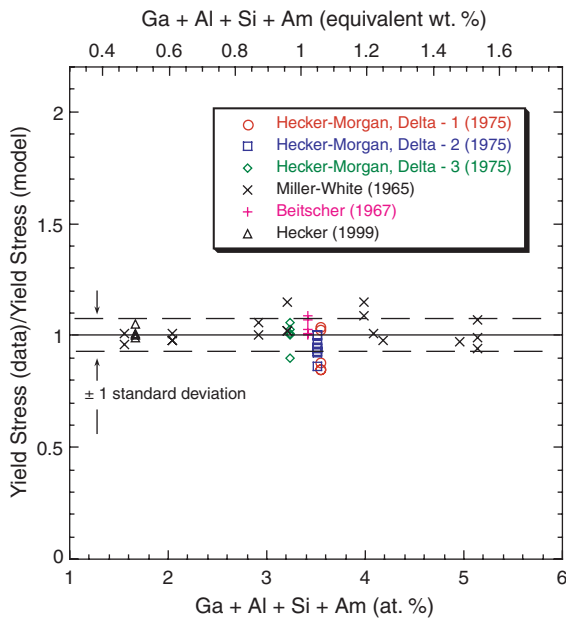


Fig. 2. The data reported in Fig. 1 normalized for grain size, strain rate, and temperature using the MTS model.

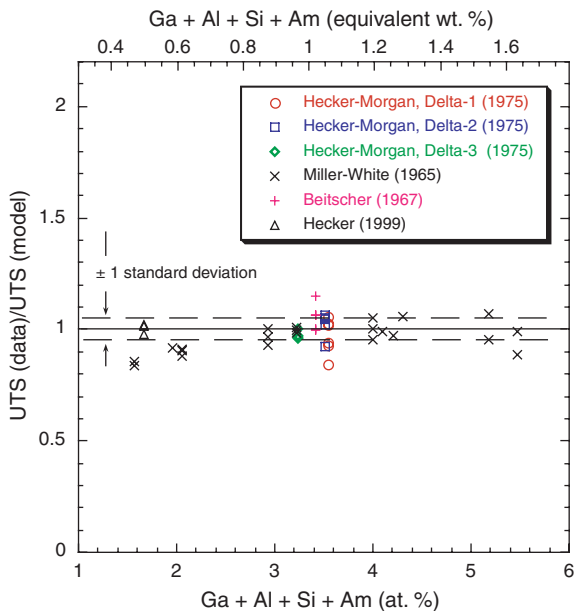


Fig. 3. A plot of the experimentally measured ultimate tensile strengths normalized by the predictions of our MTS model. The symbols indicating the origin of the data match Fig. 2.

Fig. 3 shows a similar comparison for the ultimate tensile strength. The tensile samples of Hecker and Morgan [3] and Beitscher [5] deformed to a uniform elongation of 0.18 true strain as shown in

Fig. 5 of Part I. We used our model to calculate the engineering stress associated with 20% engineering strain, 0.18 true strain, and assumed this value to be the ultimate tensile strength. To fit a hardening law, we assumed that the alloy's gallium content does not affect the work hardening behavior. Because we used data for a Pu–3.35at.%Ga alloy to construct the model, we expect agreement between the experimental and predicted ultimate tensile strengths for this composition. If gallium variations influence the hardening law, we would expect to see deviations from a horizontal line for compositions above and below 3.35 at.%.

As shown in Fig. 3, we find no deviations above 3.35 at.% Ga, but there were deviations below it. Hecker's data for a Pu–1.75at.%Ga alloy [6] fall well within 1 standard deviation, indicating that the material's work hardening is, in fact, insensitive to Ga content. The data of Miller and White [4], however, contradict this observation. These data exhibit a clear trend of decreasing ultimate tensile strength with decreasing Ga content. At this point in time, we have insufficient data to know which trend is correct.

3. Application of the model

As shown in Fig. 2, we account for differences of nearly 260% in the yield strengths of Pu–Ga alloys by normalizing the data with the MTS model to account for test temperature, strain rate, gallium concentration, and grain size. We can now use the model to specifically isolate the effects of microstructural variables such as substitutional element content, iron and nickel concentration, carbon content, and grain size.

Fig. 4 displays how gallium concentration and δ -phase stabilizing impurities – Al, Si, and Am – affect the yield strength of Pu–Ga alloys. Contributions of aluminum, silicon, and americium are quite small; the greatest sum of these elements was less than 0.27 at.% – Hecker and Morgan 'Delta-2' data [3]. The specific effects of gallium and the δ -phase stabilizing impurities on yield strength are isolated and displayed in Fig. 4 by accounting for different test conditions and grain size using the MTS model. The composition term in the model was set equal to a nominal value of 1 wt%, about 3.35 at.%. Fig. 4 shows that within the range of substitutional compositions, from 1 to 6 at.%, yield strength increases substantially with increasing alloy content. We incorporated this effect into the model in Part I by

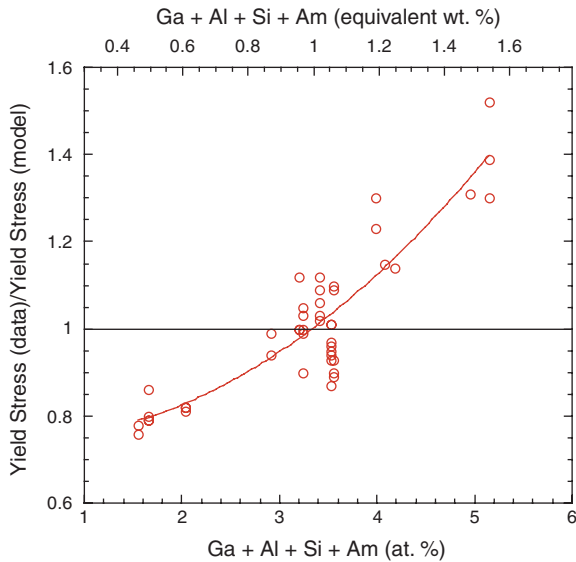


Fig. 4. Yield-strength data compensated for variations in grain size, strain rate, and temperature and normalized to a nominal composition of 3.35 at.% Ga. We show the second-order polynomial fit to these data used in Part I.

fitting these data to a second-order polynomial. This fit is shown in Fig. 4.

The range of iron and nickel impurities in the Pu–Ga alloys examined varied from undetectable amounts in electro-refined alloys to 0.08 wt% (800 wt. ppm) in low-purity alloys. In Fig. 5, we present the yield-strength data as a function of Fe + Ni content while accounting for the effects of differences in test temperature, strain rate, grain

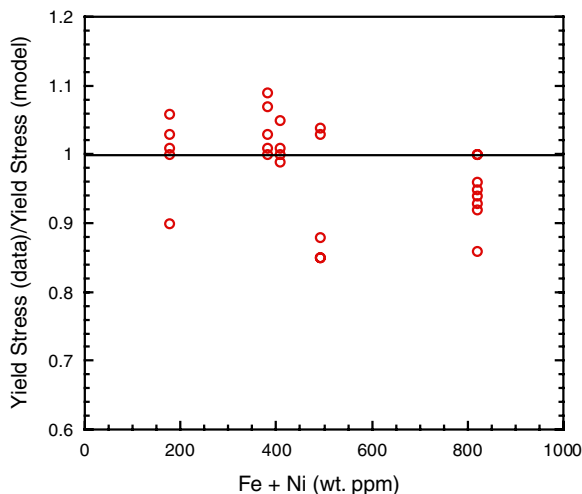


Fig. 5. Effect of iron (Fe) and nickel (Ni) impurities on normalized yield strength.

size, and solute concentration with our model. As shown in Fig. 5, there is little to no correlation between yield strength and the presence of iron and nickel in this compositional range.

At concentrations < 250 wt. ppm, iron and nickel are believed to remain in solution in the plutonium matrix. At these levels, their concentrations are very low compared to gallium concentrations. In concentrations above 300 wt. ppm, iron and nickel form low-melting-point Pu_6Fe and PuNi intermetallic inclusions, typically many microns in size as shown for a Pu–0.5wt.%Ga alloy in Fig. 6. This alloy was cast and rolled, then recrystallized, and finally homogenized. Iron and nickel intermetallic phases that appear white decorate the grain boundaries and some triple points. These inclusions would have to be nanometer size, a thousand times smaller, to effectively interact with dislocations and cause strengthening. Because of the large size of the intermetallics shown in Fig. 6, we should not be surprised that the iron and nickel content does not affect the yield strength or hardening. We do, however, expect alloys with high Fe + Ni content to affect the fracture behavior negatively [9].

Although the Fe and Ni intermetallics do not affect the room-temperature, quasi-static material strength of Pu–Ga, they can affect the mechanical behavior at high temperature. Wheeler and Robbins [2] and Beitscher [10] show that Pu–Ga alloys exhibit an extreme loss of ductility above 410 °C, where the Pu_6Fe intermetallic melts and the alloy displays hot shortness. Despite the loss of ductility, Beitscher found that there was little effect on the ultimate tensile strength. We note that the effect disappeared for Fe and Ni concentrations below 235 wt. ppm – iron and nickel below this level remain dissolved in the δ -phase lattice. The embrittlement also disappears at high strain rates, as is typical for hot-short behavior.

The materials surveyed in this study contained <350 ppm carbon. As we did for the iron and nickel, the data are normalized for all test variables and plotted as a function of carbon content in Fig. 7. We found no correlation between carbon content and yield strength in the alloys surveyed in this study. Carbon is insoluble in Pu–Ga alloys; therefore, all carbon impurities tend to form refractory precipitates. These carbides have micron dimensions, like the iron and nickel intermetallics. We believe that the large size of the carbides accounts for insensitivity of the yield strength in these alloys to carbon content.

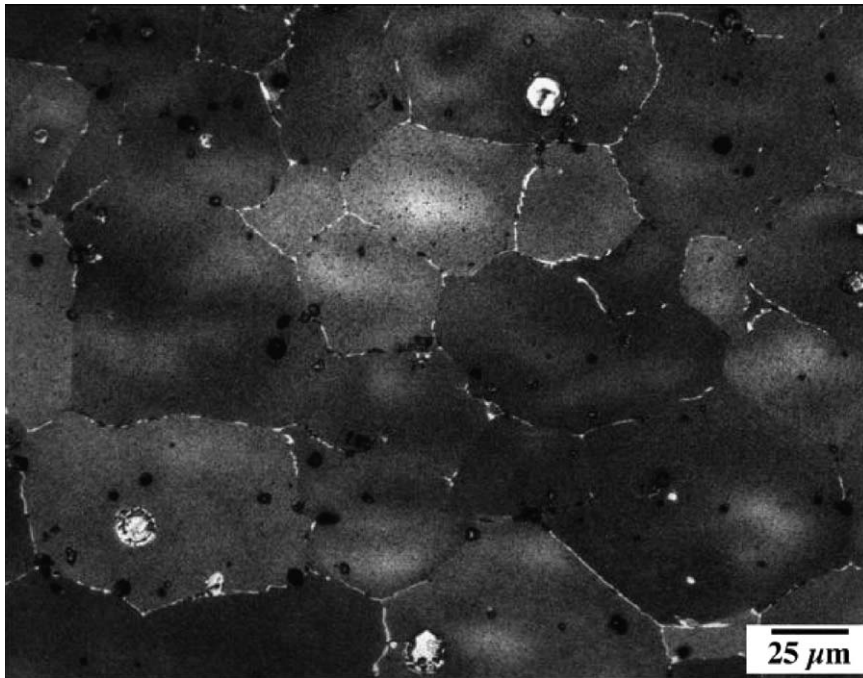


Fig. 6. Micrograph of a Pu–0.5 wt%Ga alloy containing Fe and Ni. The alloy was rolled, recrystallized, and homogenized. Note the Fe and Ni intermetallics, which appear white, decorating the grain boundaries. The intermetallics are also often prevalent at triple points. The white and black inclusions in the grain interiors are most likely carbides, oxides, and/or hydrides.

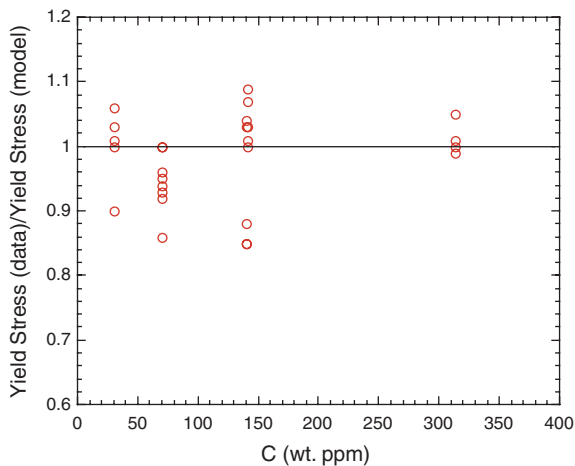


Fig. 7. Effects of carbon (C) impurities on normalized yield strength.

Wheeler et al. [11] observe that grain size affects the yield strength of plutonium–gallium alloys according to a classic Hall–Petch relationship. In Fig. 8, we compare the Hall–Petch relationship reported by Wheeler et al. with the normalized data of this report.

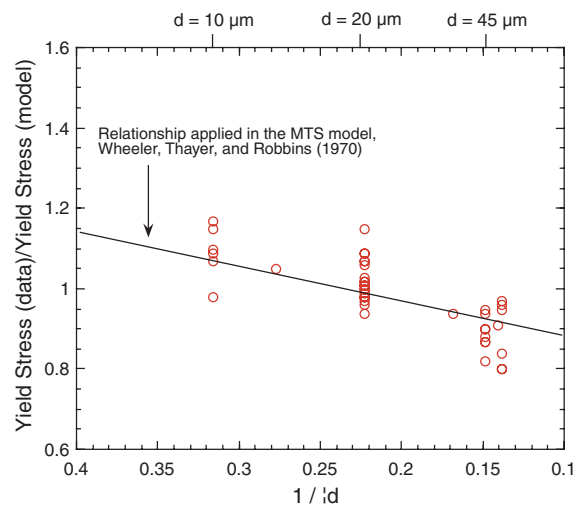


Fig. 8. Influence of mean grain size (d) in microns on yield-strength data normalized for composition, strain rate, and temperature. Data are compared to Wheeler et al.'s Hall–Petch relationship [11].

In this case, we have incorporated the effects of temperature, strain rate, and composition in the MTS model. The grain-size dimension was fixed at 20 μm , a value representative of the average grain

size of the alloys for which we have published data. The materials studied had grain sizes between 10 μm and $30 \times 90 \mu\text{m}$. The 10 μm grain size resulted from chill casting into an aluminum mold, and the non-equiaxed $30 \times 90 \mu\text{m}$ grain structure was produced by a classic rolling and recrystallization process. We note that the grain-size strengthening is small, only about 15% for the range of grain sizes considered, which is typical of other fcc metals.

4. Summary and conclusions

We validated the MTS model developed in Part I against yield and ultimate tensile strengths from approximately 50 different experiments. The predicted yield strengths agreed with the experimental data to within $\pm 7.5\%$ (± 1 standard deviation). In contrast, the variation in the original data was between 50 MPa and 130 MPa, a spread of almost 260%. Although we had to assume that the work hardening was independent of gallium concentration and grain size over the ranges examined, we successfully predicted the hardening behavior and ultimate tensile strengths, in spite of the paucity of stress/strain curves in the literature. We limited our predictions to how microstructure and composition affect yield strength because sufficient uncertainties remain in the model to predict such effects on ultimate tensile strength.

The key material variables potentially affecting plutonium–gallium alloys are gallium concentration, grain size, iron and nickel content, and carbon concentration. We predicted the yield strength of the alloys based on the temperature and strain rate of the experiment and the grain size and substitutional element concentration (Ga + Al + Si + Am). The model allowed us to plot yield strength against individual microstructural parameters to look for correlations. Grain size and gallium concentration appear explicitly in our MTS model. In these two cases, we took the input to the model as a reference value – 20 μm for grain size and 1 wt%, or 3.35 at.%, for gallium concentration.

We found that gallium concentration had the most significant effect on yield strength. We examined data for materials with a gallium content from approximately 1–6 at.%, covering almost two-thirds of the entire δ -phase field retained by gallium additions. This variation in gallium content changed the yield strength by 50%. The concentrations of impurities Al, Si, and Am, which like Ga substitute in the

fcc δ -phase Pu lattice, was small in the data sets we examined and, hence, they had negligible effects on strength.

We also found that grain size had a measurable, but modest, effect on yield strength. The experimental data we examined represented samples with average grain sizes from 10 μm to about 50 μm . Our analysis of the data confirmed the observation of Wheeler et al. [11] that the yield strength follows an inverse square-root Hall–Petch relation to grain size. The decrease of grain size from 50 μm to 10 μm produced a 15% increase in yield strength.

Lastly, we looked for a correlation between room-temperature, quasi-static yield strength and the impurity levels of iron and nickel, and carbon. We did not observe a correlation or trend in either case. The iron and nickel each form an intermetallic phase with the plutonium. Optical metallography shows that these intermetallics typically have a length scale of microns, far too large to interact effectively with dislocations and to increase the yield strength. Carbon is nearly insoluble in plutonium and forms carbide inclusions, which are also on the length scale of microns. Thus, like the iron and nickel intermetallics the carbides are too large to affect the yield strength.

The MTS model with the parameters defined in Part I can now be used to isolate the influence of test conditions and some microstructural features such as composition, grain size and inclusions content. The model will predict results beyond the current literature data so long as deformation mechanisms appropriate for the MTS model apply.

Acknowledgement

The micrograph that appears in this report was taken by Ramiro Pereyra of NMT-16, Los Alamos National Laboratory.

References

- [1] P.S. Follansbee, U.F. Kocks, *Acta Metall.* 36 (1988) 81.
- [2] A.D. Wheeler, J.L. Robbins, *J. Nucl. Mater.* 32 (1969) 57.
- [3] S.S. Hecker, J.R. Morgan, in: H. Blank, R. Lindner (Eds.), *Plutonium 1975 and Other Actinides*, North-Holland, Amsterdam, 1976, p. 697.
- [4] D.C. Miller, J.S. White, *J. Nucl. Mater.* 17 (1965) 54.
- [5] S. Beitscher, *J. Nucl. Mater.* 24 (1967) 113.
- [6] S.S. Hecker, private communication, LANL, 1999.

- [7] S.S. Hecker, D.R. Harbur, T.G. Zocco, *Prog. Mater. Sci.* 49 (2004) 429.
- [8] J.L. Robbins, *J. Nucl. Mater.* 324 (2004) 125.
- [9] S.S. Hecker, M.F. Stevens, *Mechanical Behavior of Plutonium and its Alloys*, Los Alamos Science, Number 26, 2000, p. 336.
- [10] S. Beitscher, in: W.A. Miner (Ed.), *Plutonium 1970 and Other Actinides*, Metallurgical Society of AIME, New York, 1971, p. 449.
- [11] A.D. Wheeler, W.L. Thayer, J.L. Robbins, in: W.A. Miner (Ed.), *Plutonium 1970 and Other Actinides*, Metallurgical Society of AIME, New York, 1971, p. 437.